

Research Paper

# Reversal of Vascular Calcification and Aneurysms in a Rat Model Using Dual Targeted Therapy with EDTA- and PGG-Loaded Nanoparticles

Nasim Nosoudi<sup>1</sup>, Aniq Chowdhury<sup>1</sup>, Steven Siclari<sup>1</sup>, Saketh Karamched<sup>1</sup>, Vaideesh Parasaram<sup>1</sup>, Joe Parrish<sup>1</sup>, Patrick Gerard<sup>2</sup>, Narendra Vyavahare<sup>1</sup>✉

1. Department of Bioengineering, Clemson University, Clemson, SC 29634, USA;
2. Department of Mathematical Sciences, Clemson University, Clemson, SC 29634, USA.

✉ Corresponding author: Naren R. Vyavahare, Professor and Hunter Endowed Chair, Department of Bioengineering, Clemson University, Clemson, SC 29634. Tel. No. (864) 656-5558 Fax: (864) 656-4466 Email: narenv@clemson.edu.

© Ivyspring International Publisher. Reproduction is permitted for personal, noncommercial use, provided that the article is in whole, unmodified, and properly cited. See <http://ivyspring.com/terms> for terms and conditions.

Received: 2016.06.20; Accepted: 2016.07.28; Published: 2016.08.18

## Abstract

Degeneration of elastic lamina and vascular calcification are common features of vascular pathology such as aortic aneurysms. We tested whether dual therapy with targeted nanoparticles (NPs) can remove mineral deposits (by delivery of a chelating agent, ethylene diamine tetraacetic acid (EDTA)) and restore elastic lamina (by delivery of a polyphenol, pentagalloyl glucose (PGG)) to reverse moderate aneurysm development. EDTA followed by PGG NP delivery led to reduction in macrophage recruitment, matrix metalloproteinase (MMP) activity, elastin degradation and calcification in the aorta as compared to delivery of control blank NPs. Such dual therapy restored vascular elastic lamina and improved vascular function as observed by improvement in circumferential strain. Therefore, dual targeted therapy may be an attractive option to remove mineral deposits and restore healthy arterial structures in moderately developed aneurysms.

Key words: AAA, calcification, chelation therapy, elastin, PGG.

## Introduction

Abdominal aortic aneurysm (AAA) is a balloon-like bulge in the aorta caused by thinning and weakening of the vessel wall. If AAA leads to rupture, survival rate is very low (10-15%) [1]. AAA is characterized by chronic inflammation and degradation of extracellular matrix (ECM) components by proteolytic enzymes like MMPs. This can lead to inflammatory infiltration in the adventitia and calcification and degeneration of medial elastic lamina [2, 3]. Initially, aortic aneurysms were considered to be a form of atherosclerosis, but now it is characterized as a distinct degenerative disease involving all layers of the vessel wall [1].

The infiltrating cells, including B cells, T cells, mast cells, macrophages, and neutrophils secrete proinflammatory mediators, lead to the acceleration

of matrix degradation [4]. Calcification is frequently found within the aneurysm wall, and the calcified region has a higher stiffness than the surrounding arterial wall [5]. Several drug therapies in animal models have been shown to be successful in preventing aneurysm formation, but were started at the onset of aneurysm [6]. Such studies provide insight into the mechanisms of aneurysm formation, but do not provide therapy options for already developed aneurysms. Over ninety percent of patients are diagnosed at a moderate stage of aneurysm, and therapies are critically needed to reverse these. Clinical trials with drug therapies to inhibit growth of AAA were inconclusive [6]. Currently, such patients are monitored for aneurysmal expansion by ultrasound; when the diameter of the diseased aorta

exceeds 5.5 cm, surgical replacement with a vascular graft is recommended. This threshold is arbitrary as it has been shown that at that size rupture risk exceeds interventional risk but ten percent of deaths occur below this size.

Perivascular application of calcium chloride to the infra-renal aorta of rats is a common animal model for AAA. It shows noticeable inflammatory infiltrates including macrophages and medial elastin calcification similar to that seen clinically [7]. Our group has previously shown that systemic delivery of elastin-antibody conjugated, poly (D,L-lactide) NPs loaded with hydroxamate-based MMP inhibitor batimastat (BB-94) causes suppression of AAA when delivered at the onset of disease [8]. We have also shown that EDTA-loaded bovine serum albumin (BSA) NPs with a surface conjugated elastin antibody delivered EDTA to the aneurysm site and removed calcification when applied at an early stage of the disease [9]. However, both these studies were initiated at a very early stage of the disease. To mimic the clinical situation and treat moderate-sized aneurysms, we designed this study to test if targeted NPs can regress developed aneurysms in rats. It has been previously shown that calcification is a sign of the inflammatory process involved with the degeneration of the arterial wall, and it is correlated with increased risk of aneurysm rupture [10]. Here, we used a dual-therapy approach: First, we employed targeted NPs-based delivery of EDTA to remove calcification deposits in arteries. Then, we used targeted delivery of PGG, a polyphenol known to stabilize elastin and increase elastic fiber deposition [11]. We show that such dual therapy removes mineral deposits from calcified arteries and restores elastic lamina in the aneurysmal wall, leading to improvement in vascular elastance.

## Materials and Methods

### Study Design

Sample sizes were determined by power analysis using our lab's previously published data as preliminary data. A power analysis with 90% power and  $\alpha = 0.05$  indicated that a sample size of a minimum of six rats per group was required for diameter change. Data analyses were not blinded. Outliers were not excluded.

### Preparation of DIR-loaded, EDTA-loaded, PGG-loaded NPs and EL-NP-BB94

BSA-NPs were prepared by coacervation [12]. Briefly, fluorescent infra-red dye 1, 1-dioctadecyl-3, 3, 3-tetramethylindotricarbocyanine iodide (DIR)-loaded NPs(DIR-NPs) were obtained by dissolving

250 mg of BSA (Seracare, MA) in 4 mL of deionized water. Then, 2.5 mg of DIR was dissolved in 100  $\mu$ l of acetone and added to the BSA solution. After an hour of stirring, the mixture was added dropwise to 24 mL of ethanol under continuous sonication (Omni Ruptor 400 Ultrasonic Homogenizer, Omni International Inc, Kennesaw, GA) for half an hour. For crosslinking, glutaraldehyde (EM grade 70%, EMS, PA) was added during stirring (42  $\mu$ g per mg of BSA). Next, 10 mg of DIR-NPs were incubated with 2.5 mg heterobifunctional crosslinker  $\alpha$ -maleimide- $\omega$ -N-hydroxysuccinimide ester poly (ethylene glycol) (Maleimide-PEG-NHS ester, MW 2000 Da, Nanocs Inc., NY) to achieve a sulfhydryl-reactive particle system. Traut's reagent (34  $\mu$ g, G-Biosciences, Saint Louis, MO) was used for thiolation of 10  $\mu$ g of rabbit anti-rat elastin antibody (United States Biological, Swampscott, MA), and the mixture was incubated in HEPES buffer (20 mM, pH=9.0) for an hour at room temperature. Thiolated antibodies were rinsed with HEPES buffer and were added to NPs (4  $\mu$ g antibody per 1 mg NPs) and incubated overnight for conjugation.

EDTA-loaded NPs(EDTA-NPs) were obtained by dissolving 200 mg of BSA (Seracare, MA) and 100 mg ethylenediaminetetraacetic acid disodium salt (EDTA) (Fisher scientific, NJ) in 4 mL of deionized water and pH was adjusted to 8.5. The aqueous solution was added drop-wise to 16 mL ethanol under probe sonication for 1 hour. For crosslinking, glutaraldehyde was added during sonication (10  $\mu$ g per mg of BSA). The elastin antibody conjugation procedure was similar to that of DIR-NPs.

PGG-loaded NPs(PGG-NPs) were obtained by dissolving 250 mg of BSA (Seracare, MA) in 4 mL of deionized (DI) water. PGG (125 mg) was dissolved in 400  $\mu$ l of dimethyl sulfoxide and added slowly to the BSA solution. After an hour of stirring, the mixture was added dropwise to 24 mL of ethanol under continuous sonication for half an hour. Glutaraldehyde was added during stirring at a concentration of 12 $\mu$ g/mg protein (BSA). The elastin antibody conjugation procedure was similar to that of DIR- NPs. BB-94 loaded nanoparticles (EL-NP-BB94) were prepared as previously described [8].

### In vivo study

Calcium chloride-injury model: Perivascular application of calcium chloride was used to create aneurysms in the abdominal aorta of the rats [13]. AAA and associated vascular medial calcification was allowed to develop for 30 days prior to any treatment. The diagram in Figure 1 depicts details of the animal experimentation. Briefly, Sprague-Dawley rats (5-6-weeks-old) were placed under general anesthesia

(2% to 3% isoflurane). A 0.50 mol/L CaCl<sub>2</sub>-soaked sterile cotton gauze was placed on the exposed infrarenal abdominal aorta for 15 minutes. Afterwards, the area was flushed with warm saline and sutures were used to close the abdominal incision. After surgery, the animals were given a normal diet and allowed to recover for thirty days. Either DIR dye-loaded or drug-loaded NPs were then introduced.

**Targeting and Bio-distribution of NPs:** Thirty days after the initial CaCl<sub>2</sub> injury, rats were injected with elastin antibody conjugated and DIR dye-loaded NPs (EL-NP-DIR) via the tail vein. After 24 hours, rats were euthanized. The entire body and the individual organs were imaged using a Caliper IVIS Lumina XR (Hopkinton, MA) with Ex/Em of 745/795 nm to calculate biodistribution and targeting of NPs to the site of injury in the aorta. Biodistribution was calculated with the equation below:

$$\% \text{ Biodistribution} = \frac{(\text{Fluorescence in tissue}) / (\text{Total fluorescence in all organs})}{(\text{Dry weight of tissue})} \times 100\%$$

**Reversal of moderate-size aneurysms with drug therapy:** Thirty days after perivascular application of calcium chloride, the rats were divided into four

separate treatment groups (n=6 per group). One group of rats received tail vein injection of NPs loaded with EDTA and conjugated with elastin antibody (EL-NP-EDTA, ~10 mg/kg body wt.) suspended in 200 μL of PBS twice a week; the other three groups did not receive any treatment. After the first two weeks, the EDTA-treated group received NPs loaded with PGG and conjugated with an elastin antibody once every two weeks for four weeks (EL-NP-EDTA+EL-NP-PGG ~10mg/kg body wt). The second group of six rats received NPs loaded with PGG and conjugated elastin antibody (EL-NP-PGG, ~10mg/kg body wt.) once every two weeks over four weeks. A third group of six rats received NPs loaded with BB-94 and conjugated elastin antibody (EL-NP-BB94, ~10mg/kg body wt.) once every week for four weeks. Finally, the last group of six rats received blank NPs conjugated with elastin antibody once every two weeks for four weeks (EL-NP-Blank~10mg/kg body wt.). Two weeks after completing treatment, the rats were euthanized. The entire study lasted for 12 weeks' total. After euthanasia, the tissues were harvested. They were either snap frozen or fixed in formalin for further examination. Figure 1 depicts the design of the in vivo study.

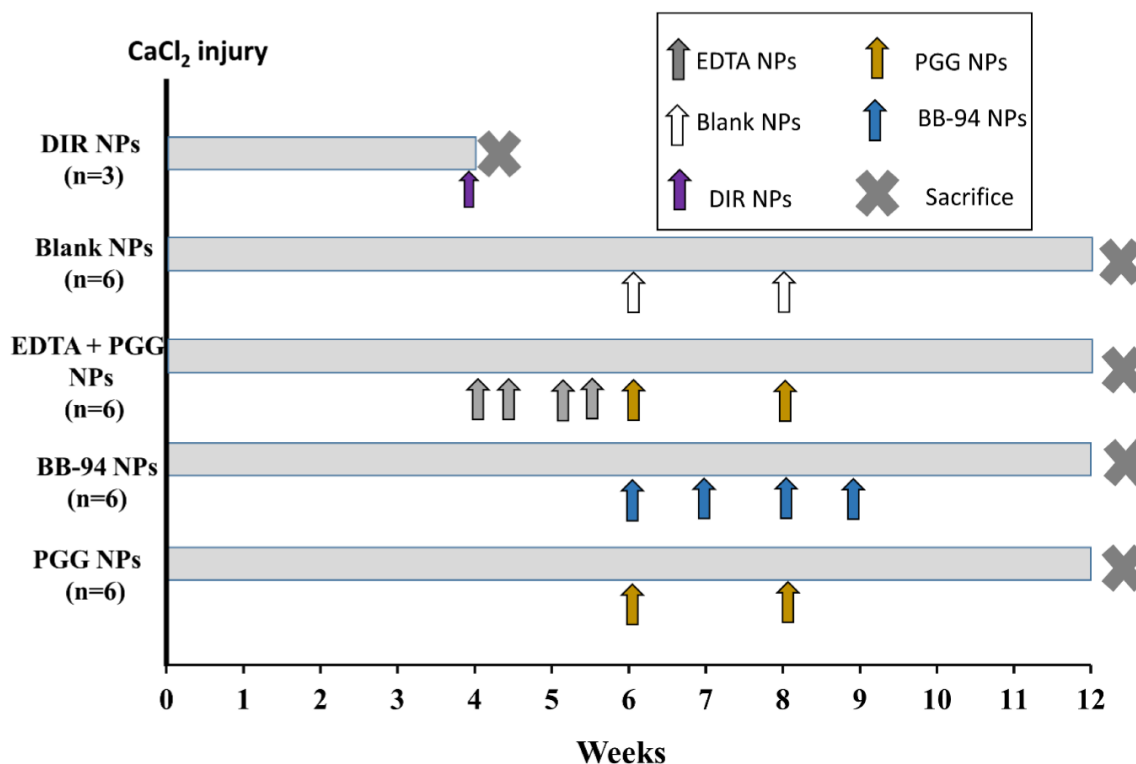


**Figure 1:** Schematic representation of the experiment. The experiment consisted of five groups (n=6 animals per group) with different NP treatments viz. DIR NPs, Blank NPs, EDTA+PGG NPs, BB-94 NPs and PGG NPs. Calcium chloride injury to the aorta was done on Day 0 following which the animals were allowed to develop aneurysm for 4 weeks. After 4 weeks, they were treated with NPs and euthanized at various chosen time points as shown in the legend. DIR NPs were administered once after 4 weeks, Blank and PGG NPs were injected twice biweekly after 6 and 8 weeks, and BB-94 NPs were injected one weekly starting at 6 weeks and through 9 weeks after injury. The EDTA+PGG NPs group was given two EDTA NP injections every week starting at 4 weeks and through 5 weeks after injury, immediately followed by biweekly PGG NP injections through 9 weeks after injury. All rats were euthanized at week 12.

### MMP activity in rat aorta and in situ zymography

The snap frozen samples of the abdominal aorta were pulverized and homogenized in RIPA extraction buffer (50 mM Tris-HCl pH 7.4, 150 mM NaCl, 1 mM EDTA, 1% Triton X-100, 1% Sodium deoxycholate, 0.1% SDS, with protease inhibitor cocktail) (Roche Diagnostic GmbH, Germany) in accordance with the manufacturer's protocol to extract protein from the aortic tissues. A BCA protein assay (Pierce, IL) was used to quantify the total protein in the harvested aortic tissue. MMP activity was measured with an internally quenched peptide substrate (excitation 280 nm, emission 360nm, MMP Substrate III, Anaspec, CA). One mg of substrate dissolved in 50  $\mu$ l of DMSO was diluted in 10 ml of development buffer (50 mM Tris Base, 5mM CaCl<sub>2</sub>•2H<sub>2</sub>O, 200mM NaCl, 0.02% brij 35). The development buffer (96  $\mu$ l) was mixed with 2  $\mu$ l of extracted protein along with 2  $\mu$ l of substrate stock solution and then incubated for an hour at 37°C. A fluorescence plate reader was used to read the endpoint fluorescence intensity.

*In situ* zymography was performed on frozen sections to evaluate MMP activity in the aortic tissue samples. Sections of the abdominal aorta obtained from sectioning with a cryostat (8  $\mu$ m) were left to air-dry for 10 min at 4° C. One part DQ-gelatin (1mg/ml of DI water) was mixed with nine parts 1% agarose (Promega, WI) in PBS containing DAPI (1  $\mu$ g/ml) (Life Technologies, IL). Each section was treated with a drop of the mixture and then incubated at 37° C for one hour in the development buffer. MMP inhibitor 1, 10-phenanthroline monohydrate (0.2 mmol/L) (Life Technologies, OR), was used to block the MMP activity of one of the samples, which was used as a positive control. Afterwards, an EVOS® XL cell imaging system was used to capture images of the samples.

### Desmosine content of the aorta

The snap frozen samples of the abdominal aorta were pulverized, lyophilized and hydrolyzed in 6N HCl at 95°C for 12 h [11]. Using nitrogen gas supplied in a continuous stream, the samples were dried. Afterwards, they were reconstituted in 1.0 mL of 0.01 N HCl. An ELISA kit (MyBioSource, San Diego) was used to measure the desmosine content in accordance with the protocol set by the manufacturer. Another group of six healthy non-injured abdominal aortas were also studied for comparison.

### Lysyl oxidase (LOX) activity assay

After being snap frozen in liquid nitrogen, the aortic tissues were pulverized and then homogenized in 500  $\mu$ l of 6 M urea, 10mM Tris (pH 7.4), 1mM PMSF

Protease Inhibitor, 1 $\mu$ M pepstatin A, and 6  $\mu$ M leupeptin. These homogenates were then placed on a plate shaker and shaken overnight at 4°C. The homogenized tissues were then centrifuged at 10,000g for 30 min at 4°C. The same buffer was used again to suspend the pellets, which were subsequently homogenized and centrifuged. Using the LOX Assay Kit (AAT Bioquest, Sunnyvale, CA) to quantify the LOX concentration in the supernatant, LOX activity was measured [14].

### Calcium Assay

Total calcium content was measured after lyophilizing. The lyophilized tissue was hydrolyzed in 6N HCl at 95°C and dried under a continuous stream of nitrogen gas (~45 minutes). The tissue was subsequently reconstituted in 0.01 N HCl and samples were analyzed using the Spectro Acros ICP Spectrometer (SPECTRO Analytical Instruments, Kleve, Germany) at Clemson University Agricultural Service Laboratory.

### Ultrasound analyses of the abdominal aorta

A high-frequency ultrasound device (Vevo 2100, VisualSonics, Toronto, Canada) utilizing a linear array probe (MS 400D, frequency 30–55 MHz) was used to image the abdominal aorta. During imaging, the animals were kept under light anesthesia by inhalation of 2% isoflurane and fixed in the dorsal position on the imaging table.

### Circumferential strain assessment with high-frequency ultrasound

Vevo 2100 analysis software was used to process M-Mode ultrasound data. Three different cardiac heart beats were recorded for each M-Mode measurement made. Systolic and diastolic diameters were measured, and this data was used to calculate the circumferential cyclic Green-Lagrange strain with the assumption that strain is uniform around the vessel according to the equation below:

$$\text{Circumferential strain} = \frac{1}{2} ((D_{\text{syst}}/D_{\text{dia}})^2 - 1) * 100\%$$

### Aortic external diameter change

Initial external diameter was measured at the time of the CaCl<sub>2</sub> injury. Final aortic diameter was recorded before euthanasia (12 weeks after injury). Additionally, we euthanized a group of rats 30 days after injury to observe diameter change at the onset of drug therapy. Aortic external diameter change was calculated as shown below:

$$\text{Aortic external diameter change \%} = \frac{\text{Final external diameter} - \text{Initial external diameter}}{\text{Initial external diameter}} \times 100\%$$

To measure aortic diameter a wooden stick of known diameter (1.99 mm) was used as a reference.

Three measurements of the aortic diameter were performed using ImageJ software for each aorta, with a wooden stick as a reference for the size.

### Histological analysis

Formalin-fixed samples were embedded in paraffin, and 5  $\mu\text{m}$  sections were mounted on glass slides and heated overnight to adhere the tissues to the slides and melt the paraffin. Subsequently, the slides were deparaffinized with xylenes and graded ethanol and stained with hematoxylin and eosin for tissue morphology, Verhoeff-van Gieson (VVG) for elastic fibers, phenol staining for PGG, Masson's trichrome for collagen and Alizarin Red S with a Light Green SF Yellowish counterstain for calcification. Liver samples were treated the same way and stained with hematoxylin and eosin for tissue morphology.

### Immunohistochemistry for macrophages, osteopontin (OPN) and vascular smooth muscle cells (VSMCs)

Tissues preserved with formalin were embedded in paraffin and sectioned as previously described. Subsequently, the slides were deparaffinized with xylenes and graded ethanol, and antigen retrieval was done using citrate buffer (Millipore, MA). The slides were incubated overnight at 4°C with the primary antibody, Mouse Anti Rat CD68 (Bio-Rad, Hercules, CA) or Rabbit Anti Rat Osteopontin (Rockland Immunochemical, PA). Staining was completed using a DAB kit (Enzo Life Sciences, NY). Slides were counterstained with hematoxylin. For vascular smooth muscle cells (VSMCs), the slides were incubated overnight at 4°C with the primary antibody, mouse smooth muscle actin (Santa Cruz Biotechnology, CA). Staining was completed using a mouse-HRP AEC kit (Enzo Life Sciences, NY). Slides were counterstained with a Light Green SF Yellowish.

### Systemic IFN- $\gamma$ levels

Blood was drawn via a heart stick with a 3 mL syringe, and after allowing 30 min for clotting, the blood was centrifuged at 3000 rpm for 3 min. Rat serum was examined for IFN- $\gamma$  using a rat ELISA kit (R&D system, MN).

### Alanine Aminotransferase (ALT) analysis

The serum was examined for the activity of alanine aminotransferase (ALT) using a commercially available kit (Sigma, St. Louis, MO).

### Statistical analysis

Data were analyzed by one-way ANOVA followed by Tukey's test. Levene's test was used to verify the homogeneity of variances and the normality assumption was checked using a

Shapiro-Wilk test. Tukey's test was used for all pairwise comparison.

An exact permutation test was performed using the NPARIWAY procedure in SAS. The data are expressed as the mean  $\pm$  standard deviation; results were considered to be significant when P-values  $\leq 0.05$ .

## Results

### NPs delivery design

Study designed was shown in Fig 1 for targeting or therapeutic purposes. BB-94 NPs were injected once a week for four weeks. PGG-EDTA NPs were injected twice a week for two weeks. PGG NPs and Blank NPs were injected once every two weeks for four weeks. These time-points for injections were chosen based on the release profile for these different agents as previously published [8, 9, 15]. There were no significant differences in  $\zeta$ -potential ( $\sim -30\text{mV}$ ) and particle size ( $\sim 200\text{nm}$ ) of NPs among different groups, viz. BB-94, PGG-EDTA, PGG, Blank and DIR NPs.

### Aortic disease status at the onset of targeted therapy

Aortic aneurysm and calcification were allowed to develop for 30 days after the initial  $\text{CaCl}_2$  injury. Aortic external diameter increased to  $127 \pm 20.6\%$  after 30 days. Desmosine content of the aortas decreased from  $1808 \pm 290.5$  to  $421.9 \pm 104$  pmole/mg dry tissue after 30 days. Calcium content of the aortas was  $43 \pm 3$   $\mu\text{g}/\text{mg}$  dry weight after 30 days. In situ zymography on frozen sections of abdominal aorta from 30 days after surgery showed high activity of MMPs (Fig 2, A1). Histological studies further corroborated quantitative data for calcification and elastin damage 30-day post-surgery (Fig 2, A2, A3).

### NP targeting to diseased aorta

Elastin antibody conjugated and DIR dye loaded NPs were injected in the tail vein at 30 days post-surgery. The NPs targeted the injured aortic elastic lamina sites within the first 24 hours as measured by fluorescence intensity (IVIS,  $42 \pm 22\%$  targeting based on per weight basis) (Fig 2 B). The fluorescence signal of DIR (% fluorescence/dry weight of organ) after 24 hours was  $3.6 \pm 1.5\%$  for the kidneys,  $20 \pm 7\%$  for the liver, and  $20 \pm 14\%$  for the spleen (Fig 2C). More significantly, infiltration of the NPs was seen from the adventitial side to the medial section, where elastin was found to be degraded (Fig 2D). In a previous study, we have shown that once NPs get to the injury site, they stay up to 14 days at the site (data not shown). Based on this information we chose to inject drug loaded NPs every two weeks for the therapeutic studies.

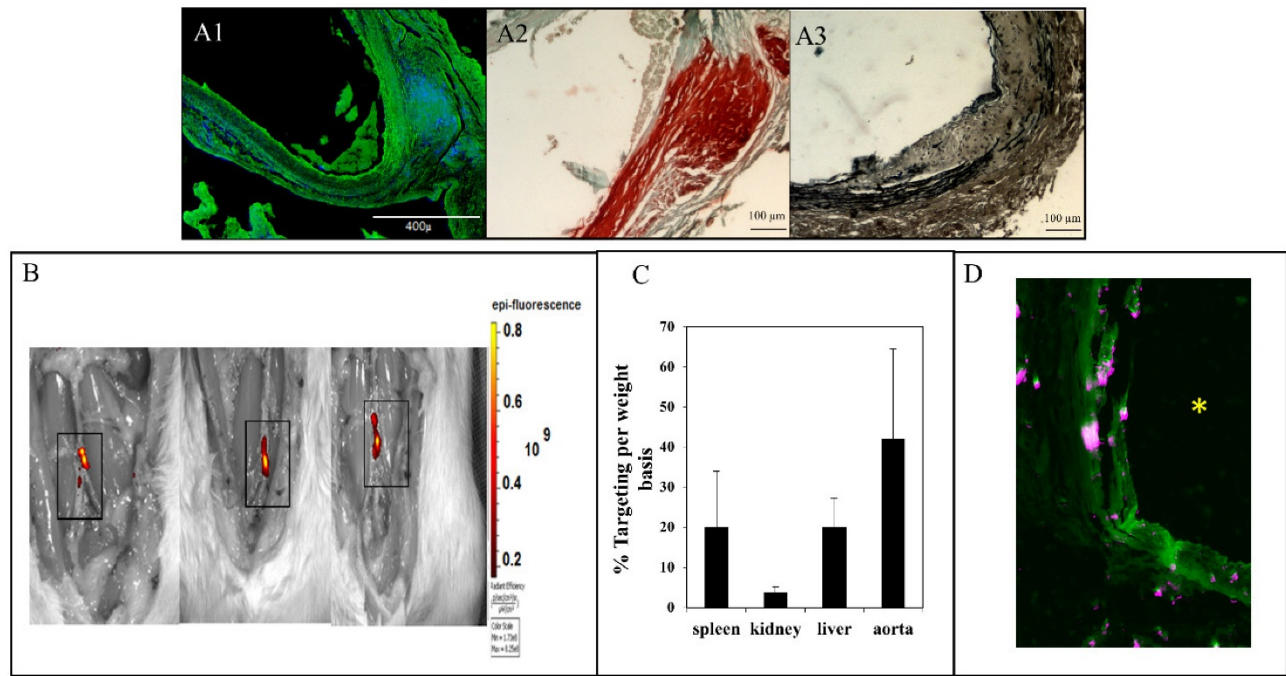
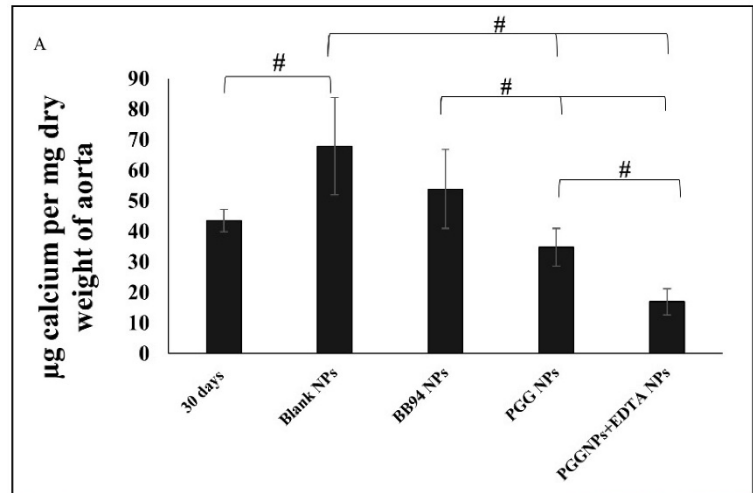


**Figure 2:** In situ zymography for MMPs (A1), alizarin red staining for calcium (A2) and VVG staining for elastin (fibers stained black) (A3) for aortic samples 30 days after injury. In situ zymography confirmed the high activity of MMPs (-9 and-2). Alizarin red confirmed calcification in the media and adventitia. VVG showed the elastin damage. (B) NP accumulation after intravenous injection of EL-NP-DIR, 30 days after injury at the site of elastin damage (squares show sections of the abdominal aorta where CaCl<sub>2</sub> was applied); image taken 24 hrs after injection. (C) Organ distribution of fluorescent NPs 24 hrs after injection of EL-NP-DIR. (D) Cross-section of abdominal aorta showing NPs (EL-NP-DIR) targeting from the adventitial side and accumulating more in the degraded elastic lamina; DIR fluorescence (purple) and elastin (green autofluorescence). \* indicates lumen.

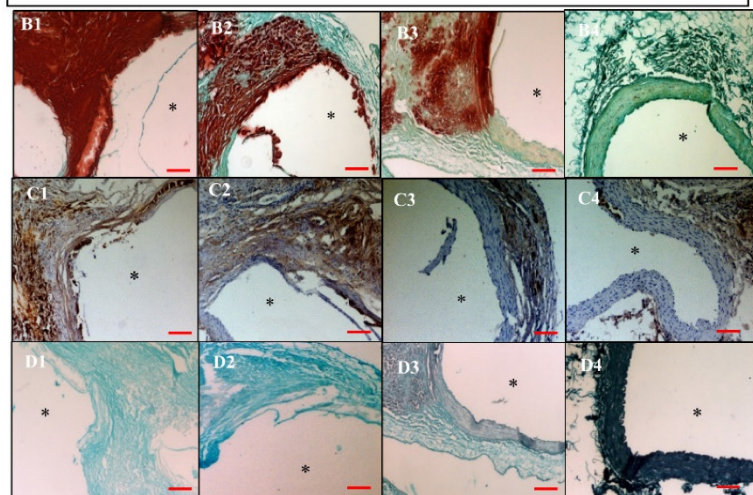
**Figure 3:** Calcium content of aorta 30 days after injury and before any treatment compared to EL-NP-Blank group, EL-NP-BB94 group, EL-NP-PGG group and EL-NP-EDTA+EL-NP-PGG groups (#P < 0.05, Tukey's test.) (n=6). Alizarin red staining (calcium) with a Light Green SF Yellowish counterstain for the EL-NP-Blank group (B1), EL-NP-BB94 group (B2), EL-NP-PGG group (B3), and EL-NP-EDTA+EL-NP-PGG group (B4) shows high calcification (B1, B2); mild calcification (B3); minimal calcification (B4). OPN IHC revealed higher OPN expression in the EL-NP-Blank and EL-NP-BB94 groups (C1, C2); less OPN expression in the EL-NP-PGG group and EL-NP-EDTA+EL-NP-PGG groups (C3, C4). For histological confirmation of PGG binding to elastic lamina, all groups' sections were stained with a phenol-specific stain (black indicates PGG) and counterstained with Light Green SF Yellowish, showing no staining for EL-NP-Blank (D1) and EL-NP-BB94 (D2); mild phenol staining close to the elastic lamina in the EL-NP-PGG group (D3); very strong staining in the EL-NP-EDTA+EL-NP-PGG group (D4). \* indicates lumen. Scale bar is 100 μm.



## Dual therapy for calcified aneurysms

### Calcification assessment

When blank NPs (EL-NP-Blank) or NPs loaded with an MMP inhibitor BB-94 (EL-NP-BB94) were delivered, aortic calcification continued to increase (67.80±16 μg and 53.82±12.97 μg calcium /mg dry weight of aorta respectively). When only PGG NPs (EL-NP-PGG) were delivered, aortic calcification did not increase, but remained similar to the aorta 30 days post CaCl<sub>2</sub> injury (34.8±6 μg calcium /mg dry weight of aorta). Only when delivery of EDTA NPs was followed by PGG NPs, we found a significant reduction in calcification (16.8±4.2 μg calcium /mg dry weight of aorta). (Fig 3A)



Alizarin Red S staining for calcification with a Light Green SF Yellowish counterstain showed very heavy calcification in the EL-NP-Blank (Fig 3B1) and EL-NP-BB94 groups (Fig 3B2), especially in the media and adventitia. Calcification was moderate in the EL-NP-PGG group (Fig 3B3). Calcification was minimal to nonexistent with dual therapy where EL-NP-EDTA was administered followed by EL-NP-PGG (Fig 3B4).

Immunohistochemical(IHC) staining for osteopontin (OPN) was positive in the EL-NP-Blank (Figure 3C1) and EL-NP-BB94 (Figure 3 C2) groups and co-localized with high calcification in the medial layers. OPN was observed, but was not abundant in the other groups (Figure 3C3 and C4).

We used FeCl<sub>3</sub> stain to look at PGG binding to elastin. As expected, no phenol staining (black-gray for PGG) was seen in the EL-NP-Blank and EL-NP-BB94 groups (Fig 3D1 and D2). Staining was intense in the EL-NP-EDTA+EL-NP-PGG group (Fig 3D4) as compared to the EL-NP- PGG group (Fig 3D3), suggesting a higher amount of PGG attached to elastin after removal of mineral deposition by EDTA.

### Aortic external diameter change

Aortic external diameter increased from 127±20.6% to 185±25% when control blank NPs were injected (EL-NP-Blank), suggesting that targeted blank NPs did not inhibit aneurysmal growth (Figure 4A, B). However, when EL-NP-PGG or EL-NP-EDTA+EL-NP-PGG NPs were injected, a significant suppression of aortic external diameter change was observed (66±21% and 25±7% respectively). Moreover, NP delivery of BB94 (EL-NP-BB94) showed no reversal of aortic external diameter expansion (156±17%) (Fig 4).

### MMP Activity and in situ zymography

We examined if delivery of NPs loaded with PGG, BB-94 or EDTA followed by PGG would inhibit local MMP activity at the injury site. Fluorescence intensity data normalized to total protein content showed highest activity in the EL-NP-Blank group, clearly suggesting that blank NPs did not reduce MMP activity. All other groups (EL-NP-PGG, EL-NP-BB94, and EL-NP-EDTA + EL-NP-PGG) showed significant suppression of MMP activity (Fig 5A). In situ zymography confirmed the quantitative results (Fig 5B).

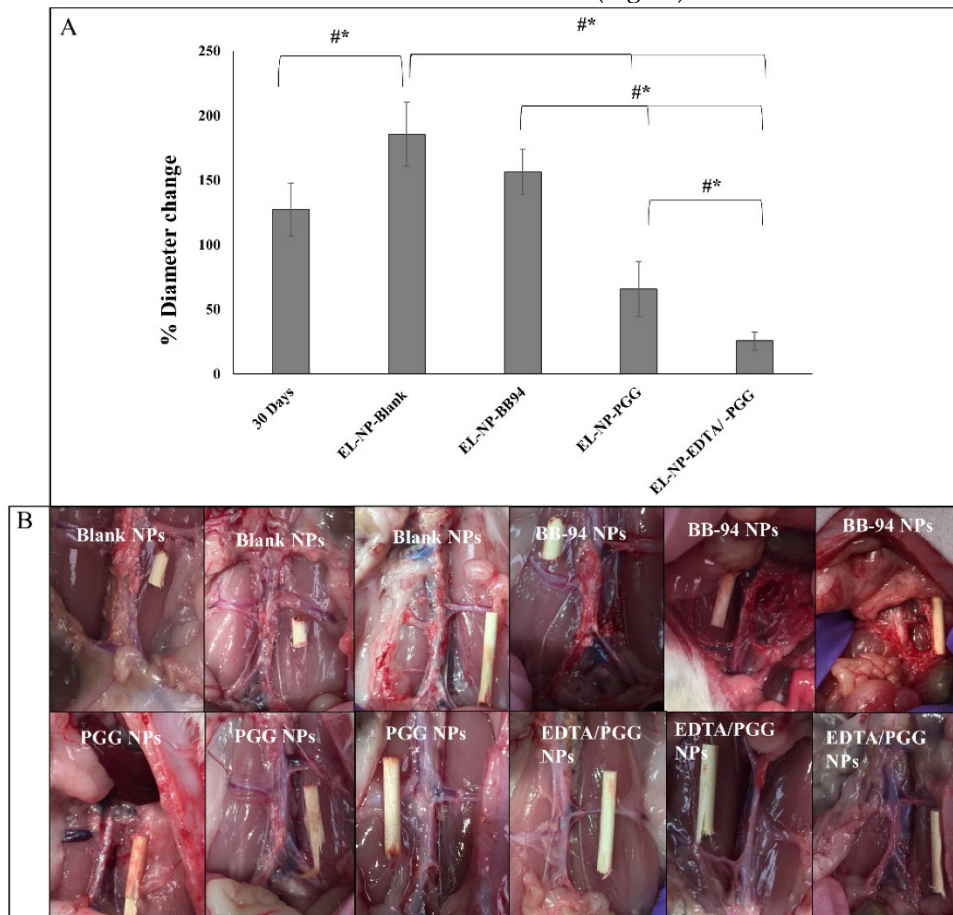


**Figure 4:** Comparison of aortic external diameter change shows a significant suppression of AAA expansion in the EL-NP-EDTA+EL-NP-PGG group compared to all other groups (A). 30 days represents aortic diameter at the initiation of treatments. Representative images of the aorta at sacrifice (B). Wooden sticks were kept as reference for external diameter change measurement. \*, P < 0.05 represents statistical significance, Tukey's test (pairwise comparison). #, P < 0.05, Exact permutation test. (n=6).

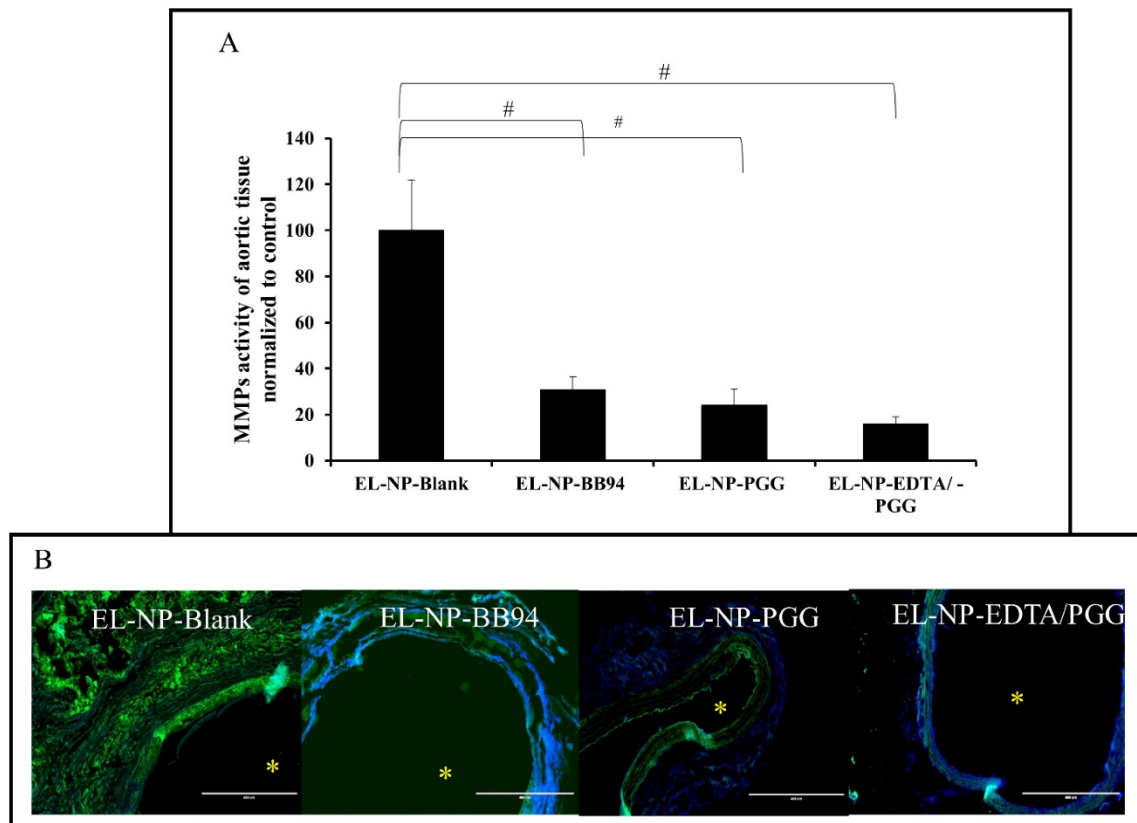


**Figure 5:** (A) MMP activity (-2 and -9) as measured by a fluorogenic substrate assay showing increase in MMP activity in the EL-NP-Blank group abdominal aorta compared to all other groups. MMPs were not inhibited in the abdominal aorta by blank NPs, while they were suppressed in other groups. (B) MMP activity in abdominal aortic sections shown with *in situ* zymography. Green signal: active MMPs; blue signal: DAPI staining for cell nuclei. Only the EL-NP-Blank group shows MMPs activity. \* Indicates lumen. Scale bar = 400  $\mu$ m. (#P < 0.05, Tukey's test.) (n=6).

### Histological analysis: aortic inflammation

Hematoxylin and eosin staining in the EL-NP-Blank and EL-NP-BB94 groups showed significant adventitial inflammation with large macrophage infiltration in the media (Fig 6a and b). Minimal inflammation was seen in the EL-NP-EDTA+EL-NP-PGG group (Fig 6d). Masson trichrome staining revealed that collagen deposition was abundant in the EL-NP-Blank (Fig 6e) and EL-NP-BB94 (Fig 6f) groups while muscle fibers were minimal. Collagen deposition was lower in the EL-NP-PGG group (Fig 6g) and minimal in the EL-NP-EDTA+EL-NP-PGG group (Fig 6h).

### Immunostaining for macrophages (CD68) and VSMCs

The EL-NP-Blank group (Figure 6i) showed adventitial granuloma and intense pan-macrophage (CD-68) staining. In the EL-NP-BB94 (Figure 6j) and EL-NP-PGG (Figure 6k) groups, the adventitia stained positive for pan-macrophages, but with lower staining than the blank NPs group. The EL-NP-EDTA + EL-NP-PGG group had the least amount of CD68 staining (Figure 6l). Depletion of medial VSMCs was observed in both the EL-NP-Blank (Figure 6m) and

EL-NP-BB94 (Figure 6n) groups, while more medial VSMCs were found in the EL-NP-PGG (Figure 6o) and EL-NP-EDTA + EL-NP-PGG (Figure 6p) groups.

### Systemic IFN- $\gamma$ levels

The EL-NP-Blank group had the highest amount of IFN-  $\gamma$  (23.7 $\pm$ 7.6 pg/ml) in serum, followed by the EL-NP-BB94 group (11.2 $\pm$ 4.8 pg/ml). IFN-  $\gamma$  levels in the dual therapy group (EL-NP-EDTA + EL-NP-PGG) and EL-NP-PGG group were below detectable levels.

### Restoration of elastic lamina:

We tested if drug therapy restored already degraded elastic lamina. LOX enzyme activity and desmosine content was measured, and VVG histological staining for elastic lamina was also done. We also tested circumferential strain with ultrasound at the end of the study.

**LOX activity:** LOX analysis of abdominal aortic samples, as measured by ratio of thoracic aorta of the same animal showed a significant decrease in LOX in the EL-NP-Blank and EL-NP-BB94 groups, suggesting elastin crosslinking was inhibited. However, the EL-NP-PGG and EL-NP-EDTA + EL-NP-PGG groups showed a significant increase in LOX activity (Figure 7A).

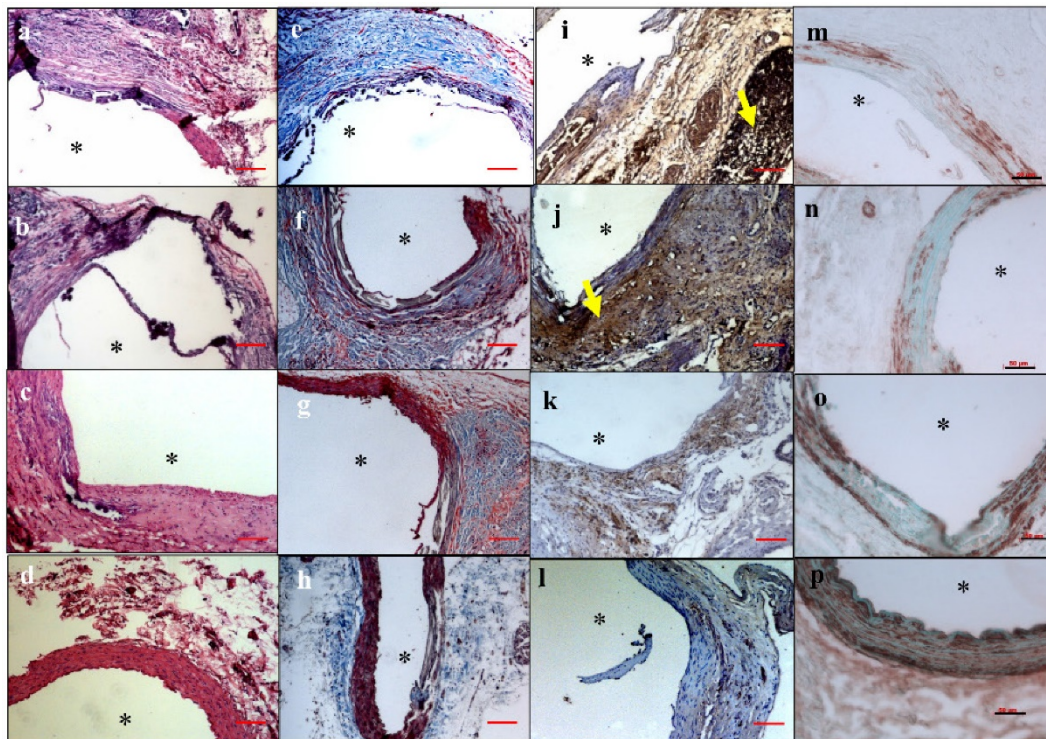


**Figure 6:** Hematoxylin and eosin (H&E) staining showed inflammation in the EL-NP-Blank (a), EL-NP-BB94 (b), and EL-NP-PGG (c) groups, while inflammation was minimal in the EL-NP-EDTA+EL-NP-PGG (d) group. Masson trichrome staining showed excess collagen deposition in the EL-NP-Blank (e) and EL-NP-BB94 (f) groups, while it was minimal in the EL-NP-PGG (g) and EL-NP-EDTA+EL-NP-PGG (h) groups. CD68 macrophage IHC was positive for the inflammatory capsule in the EL-NP-Blank (i) and EL-NP-BB94 (j) groups. CD68 expression was minimal in the EL-NP-PGG (k) and EL-NP-EDTA+EL-NP-PGG (l) groups. VSMC expression was higher in the EL-NP-EDTA+NP-PGG (p) group compared to the EL-NP-Blank (m), EL-NP-BB94 (n), and EL-NP-PGG (o) groups. \* Indicates lumen. Red scale bar is 100 μm. Black scale bar is 50 μm.

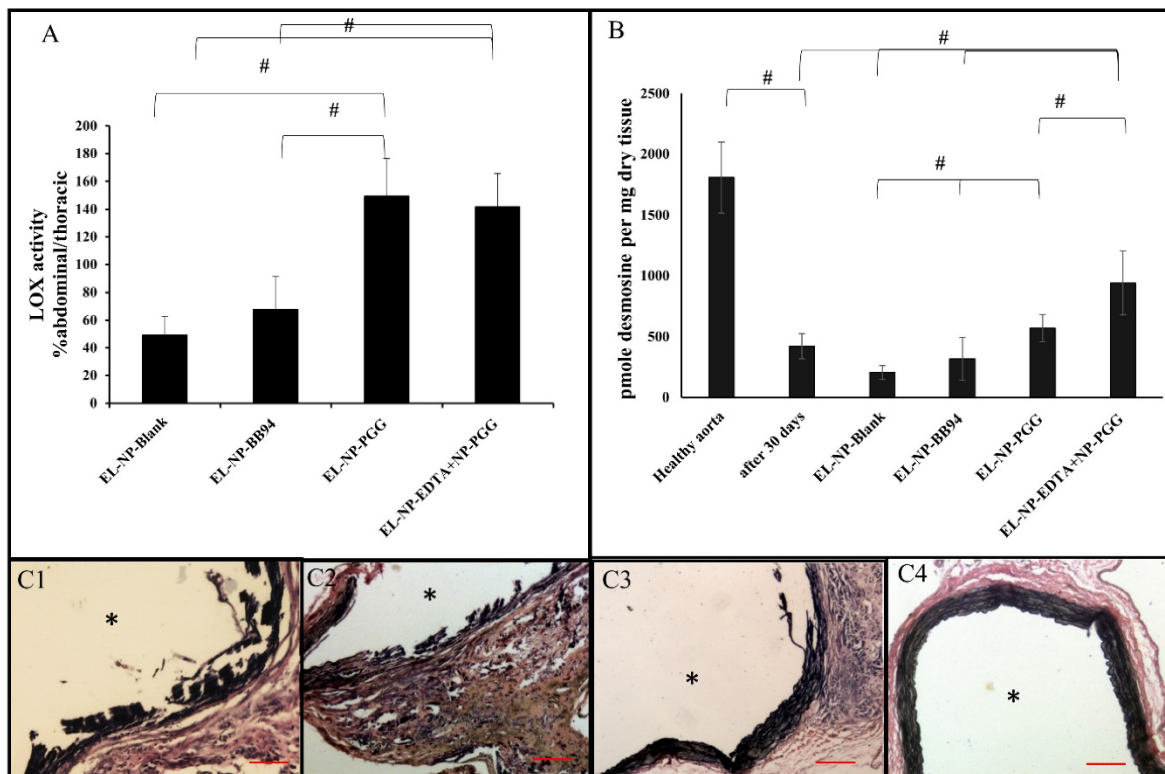


**Figure 7:** (A) LOX activity in the abdominal part (CaCl<sub>2</sub> injured) over the thoracic aorta (non-injured, healthy), showing that LOX activity was reduced in the EL-NP-Blank and EL-NP-BB94 groups. The EL-NP-PGG and EL-NP-EDTA+EL-NP-PGG groups showed increased LOX; both are significantly higher than the EL-NP-Blank and EL-NP-BB94 groups. (B) Desmosine content of aorta 30 days post injury and in the four NP groups was compared to healthy non injured abdominal aorta. CaCl<sub>2</sub> injury caused a substantial decrease in desmosine. Desmosine content was not improved after delivery of blank or BB-94 loaded NPs (EL-NP-Blank or EL-NP-BB94). The EL-NP-EDTA+EL-NP-PGG group showed the highest desmosine content among the four groups.

**Desmosine content:** Desmosine content of abdominal aortic samples in the EL-NP-Blank group was further reduced from  $421.9 \pm 104$  to  $205 \pm 56$  pmole desmosine/ mg dry tissue, suggesting further elastin degradation. The EL-NP-BB94 group had  $317 \pm 177$  pmole desmosine/ mg dry tissue, suggesting BB94 treatment also did not prevent elastin degradation (no significant differences between the EL-NP-BB94 and EL-NP-Blank groups). Desmosine content in the EL-NP-PGG group was significantly higher than in the EL-NP-Blank group ( $571 \pm 113$  pmole desmosine/ mg dry tissue). The EL-NP-EDTA + EL-NP-PGG group had the highest amount of desmosine among the four groups ( $940 \pm 261$  pmole desmosine/ mg dry tissue), clearly showing increased elastic lamina crosslinking. A healthy non-injured aorta has  $1808 \pm 290.5$  pmole desmosine/ mg dry tissue (Fig 7B).

**VVG stain for elastic lamina:** Histological evaluation of elastic lamina further confirmed the quantitative results. VVG staining for elastic lamina in aortic sections showed severe damage in the EL-NP-Blank (Fig 7C1) and EL-NP-BB94 (Fig 7C2) groups, while the elastic lamina was partially damaged in the EL-NP-PGG (Fig 7C3) group. However, elastic lamina had a natural wavy pattern as seen in healthy aortas in the dual therapy group (EL-NP-EDTA + EL-NP-PGG) (Fig 7 C4).

Verhoeff-van Gieson (VVG) staining revealed that the elastic lamina was fragmented and damaged in the EL-NP-Blank and EL-NP-BB94 groups (C1), (C2), while the elastic lamina was partially restored in the EL-NP-PGG (C3) group and was restored very well in the EL-NP-EDTA+EL-NP-PGG (C4) group.

(#P < 0.05, Tukey's test,) (n=6). \* Indicates lumen. Scale bar is 100  $\mu$ m.

**Circumferential strain:** Healthy aorta circumferential strain was  $\sim 13.7 \pm 1.5\%$  (n=6). In this study, we measured circumferential strain at two time points, 30 days after injury (before any treatment began (week 4)) and week 12 (after the treatments finished and before euthanasia) (Fig 8). We have shown both values for each group and compared week 4 with week 12 in each group. At 30 days after CaCl<sub>2</sub> injury, there was a significant decrease in circular strain in abdominal aortas, suggesting stiffening of the artery due to loss of elastin, deposition of collagen, and aortic mineralization. The EL-NP-Blank and EL-NP-BB94 group did not show any significant improvement in these values after 8 weeks of treatment, while both PGG groups (EL-NP-PGG) and (EL-NP-EDTA+EL-NP-PGG) showed significant improvement in circumferential strain, suggesting that elastin regeneration helps restore aortic biomechanics.

#### Liver function: Alanine Aminotransferase (ALT) analysis

Serum ALT, an enzyme used to assess liver function, was consistently within the acceptable range of 5-to-45 U/L ( $7.8 \pm 0.5$  U/L for EL-NP-Blank,  $6.4 \pm 0.1$  U/L for EL-NP-BB94,  $5.2 \pm 0.6$  U/L for EL-NP-PGG, and  $6.7 \pm 0.5$  U/L for EL-NP-EDTA + EL-NP-PGG rats). No differences were observed in liver histological sections stained with hematoxylin and eosin, suggesting that our treatment did not have any toxic effect on the liver (data not shown).

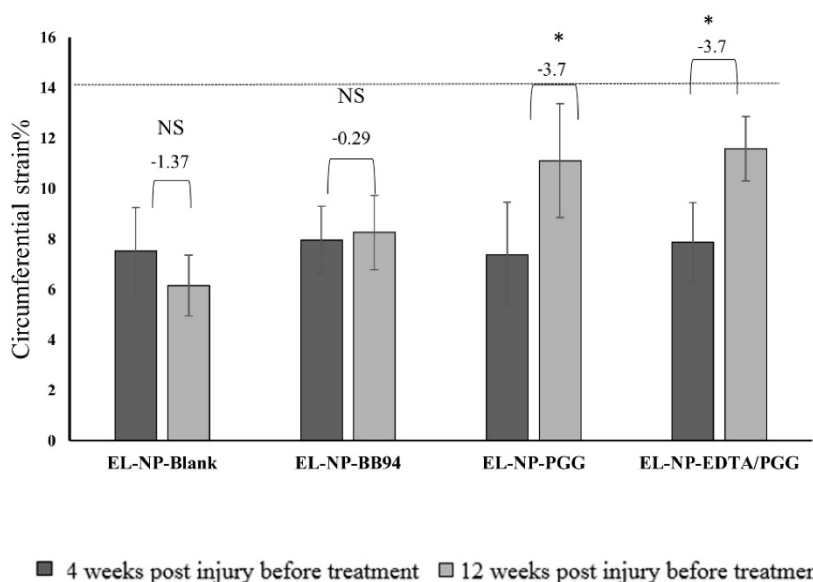


**Figure 8:** Circumferential strain as measured by ultrasound of all four groups at week 4 after injury and before any treatment compared to week 12 after treatments. No differences (NS) were observed in the EL-NP-Blank and EL-NP-BB94 groups while in both the EL-NP-PGG and EL-NP-EDTA+EL-NP-PGG groups there was a significant enhancement. (\*P < 0.05, Tukey's test,) (n=6). Dashed line shows the circumferential strain in a healthy rat with no injury.

## Discussion

The ultimate goal of pharmacological therapy for AAA is to promote regression of the disease and decrease the chance of surgery and rupture. Different medications, like statins, angiotensin-converting enzyme (ACE) inhibitors, angiotensin receptor blockers and inhibitors of MMPs were tested in animals' studies [6]. However, these pharmacological treatments were started at the onset of AAA induction, and these drugs reduced either inflammation or enzyme activity, but were unable to restore ECM milieu.

Our group is working on nanoparticle-based targeted therapy for AAA that can halt or regress the disease with pharmacological agents. In our previous work, we have shown that an MMP inhibitor like BB-94, if targeted early, can halt the progression of AAA in a rat model [8]. Similarly, we have shown that EDTA targeting can remove early mineral deposits in a CaCl<sub>2</sub> injury rat model [9]. Both treatments were initiated near the start of the disease. However, pharmacological therapies cannot be preemptively used in patients as a precautionary measure. Once diagnosed, patients will already have developed aneurysm. Therefore, in this study, we validated the combinational use of targeted NPs carrying a chelating agent to remove calcification followed by delivery of PGG, a potent elastin protectant to reverse already developed calcified aneurysms in rats. We included delivery of BB-94, an MMP inhibitor to test if merely suppressing further degradation of ECM restores the degraded elastic lamina.

Different degrees of calcification are present in most AAAs [16]. Systemic EDTA therapy has been touted and used in many countries to improve vascular function, but it is still controversial [17]. A recently concluded clinical trial (TACT) of systemic therapy for coronary disease showed slightly improved cardiovascular function that did not reach statistical significance and is therefore not FDA-approved [18]. Systemic EDTA therapy can chelate calcium in the serum and can also lead to bone loss and hypocalcemia [17]. Our approach of targeted EDTA therapy requires a 20-times-lower dose of the chelating agent that is encased in a nanoparticle and is specifically targeted to elastin calcification sites. In this study, we show that advanced calcification (30 days after injury) can be removed by targeted NP-based EDTA therapy. As expected, delivery of blank NPs did not inhibit calcification progression. Importantly, BB-94 delivery, although successful in inhibiting MMP activity at the site of AAA, was unable to prevent further calcification of the aorta. These data clearly show that suppression of a

degradation pathway alone is insufficient to regress an aneurysm or existing calcification. When PGG NPs were delivered, we saw inhibition of further calcification. PGG has an affinity for proline-rich proteins like collagen and elastin, allowing for the formation of hydrogen bonds [19]. It has been shown that amino and carboxyl groups are potential nucleation site for calcification on elastin [20]. PGG has many phenolic hydroxyl groups, and they can interact with these binding sites and form hydrogen bonds. In this way, nucleation sites for calcium binding may have been blocked, and therefore elastin was protected from further calcification. Phenolic staining confirms PGG binding to elastin. This shows that even though PGG does not have the ability to remove calcium, it can protect elastin and possibly make a hydrogen bond and block nucleation sites on elastin. Strikingly, when we used EDTA NPs first to remove mineral deposits and then applied PGG NPs in a sequential manner, we saw not only suppression of further mineralization, but regression of deposited mineral. After EDTA treatment, we saw a higher amount of PGG binding to the elastin, which led to blocking calcification and degradation sites. Others have shown that OPN is abundant in calcified tissue and is an important regulator of arterial mineral deposition [21]. Moreover, it has been confirmed that the aortic tissues of aneurysmal patients have more OPN than non-aneurysmal patients [22]. In this study, OPN levels in the tissue correlated with the extent of calcification: The highest OPN content occurred in the blank NP group, and the lowest in the dual therapy group.

Inflammation with macrophage infiltration is an important feature of AAA [23]. Pan-macrophage presence at the site of injury was abundant in the EL-NP-Blank and EL-NP-BB94 groups. MMP inhibitor BB-94 was unable to reduce inflammatory conditions. When PGG alone was delivered (EL-NP-PGG group), we saw significant reduction in macrophage presence. However, when EDTA therapy was followed by PGG (EL-NP-EDTA+EL-NP-PGG group), a complete lack of macrophage presence was seen. It is known that elastin fragments (EFs) or elastin degradation products (EDPs) at the site of injury are chemotactic to macrophages, and this mechanism is mediated by elastin binding proteins [24]. Thus, suppression of elastin degradation may have further led to suppression of macrophage activity in the area and significant suppression of MMP activity in the PGG groups. Another reason for suppression of macrophages in the EL-NP-EDTA+EL-NP-PGG group may be reduction in calcification. It has been shown that OPN is a potent chemotactic factor for macrophages [25]; we saw reversal of OPN

expression after removal of mineral, and this may have also lead to suppression of macrophages. CaCl<sub>2</sub>-mediated aneurysm was accompanied by depletion of the medial layer of smooth muscle cells, which others have reported [26]. In the EL-NP-blank, EL-NP-BB94 and EL-NP-PGG groups, we found depletion of VSMCs where the elastin was damaged. Higher staining for viable VSMCs was observed in the dual therapy group (EL-NP-EDTA+EL-NP-PGG group), probably due to removal of mineral deposits and lowering of inflammatory milieu in the aorta.

Systemic inflammation was tested by looking at serum IFN- $\gamma$  levels in rats. IFN- $\gamma$  was detected in the serum of AAA patients; additionally, AAA sections and tissue extracts from mice contained high levels of IFN- $\gamma$  [27]. We observed a higher level of IFN- $\gamma$  in serum of the EL-NP-Blank and EL-NP-BB94 groups compared to the EL-NP-PGG and EL-NP-EDTA+EL-NP-PGG groups. This clearly suggests suppression of local inflammation led to suppression in systemic inflammatory markers.

Next, we looked at the elastin content of the aorta after the targeted therapy. We have shown earlier that PGG treatment of vascular smooth muscle cells from aneurysmal aortas in culture shows enhanced deposition of insoluble elastin fibers [28]. We hypothesize that due to PGG's multifunctional nature, when it binds to degraded elastin in the ECM, it has additional binding sites that can bind and anchor soluble tropoelastin precursors secreted by cells. This in turn can lead to increased LOX enzyme synthesis by cells to crosslink the tropoelastin. LOX is an important enzyme in elastin fiber assembly that facilitates covalent crosslinking of elastin precursors by oxidizing peptidyl lysine to amino adipic semialdehydes [29]. It has been shown that reduced LOX activity is involved in the pathogenesis of AAA [30, 31]. As expected, aneurysmal aorta in the blank NP group showed significantly lower LOX activity as compared to healthy thoracic aorta. Delivery of BB94 did not change LOX activity, suggesting that expression of MMPs and LOX are independently controlled. When PGG was delivered either alone or after EDTA therapy, we saw significant increases in LOX activity similar to previous data from in vitro cell cultures [28].

We also looked at the desmosine content of the aorta, another marker for elastin maturation. It has been shown that levels of desmosine are significantly lower in aneurysmal specimens from human patients with AAA [32, 33] than in controls, suggesting loss of mature crosslinked elastin. In our AAA model, we also observed a significant loss of desmosine as compared to healthy aorta levels, suggesting elastin degradation at the site of injury in the blank NP and

BB94-NP groups. When PGG was delivered, we observed an increase in desmosine content in the aneurysmal aorta. Moreover, in the dual therapy group (EL-NP-EDTA /EL-NP-PGG) desmosine content was significantly higher than in the PGG group alone. This suggests that calcification can be a burden to elastin regeneration; when calcium was removed by EDTA delivery, elastin regeneration was facilitated. Our histological evaluation of elastin lamina with VVG staining corroborated LOX and desmosine data, showing wavy intact elastic lamina in the dual therapy group only, clearly showing regeneration of medial elastic layers after dual therapy.

We next looked at whether elastin regeneration led to improvement in tissue biomechanical parameters. It has been shown that loss of circumferential strain is the result of aneurysmal aortic degeneration [34]. Circumferential strain decreased in the EL-NP-Blank group, suggesting stiffening of the aorta. There was a very small increase in the EL-NP-BB94 group, but this increase was not statistically significant compared to the EL-NP-Blank group. Circumferential strain was increased after treatment with PGG alone and with dual therapy of EDTA and PGG (EL-NP-PGG and EL-NP-EDTA+EL-NP-PGG groups) suggesting that the functionality of the aorta in terms of elastance can be restored by elastin regeneration. Aneurysmal development as assessed by external diameter of aorta had progressed unhindered in blank NP and BB94-NP groups. Delivery of PGG led to aneurysmal regression compared to the EL-NP-Blank and EL-NP-BB94 groups. The EL-NP-EDTA+EL-NP-PGG group completely reversed aneurysmal dilation, and the aorta size was equivalent to the healthy aorta, suggesting that the combinational treatment of removing calcium by EDTA and regenerating elastin by PGG treatment may be the best strategy to reverse the disease.

A significant portion of NPs in this therapy go to the kidneys, spleen, and liver. We observed a significant decrease in NP content in the liver and kidneys two weeks after injections (data not shown). Thus, we hypothesize these NPs are cleared by the reticuloendothelial system (RES system) [35]. We looked at ALT levels in the livers of treated rats. The ALT enzyme is the most sensitive indicator of hepatic injury [36]. The ALT level was the same among the four groups, and livers appeared normal in histological sections, suggesting that NPs were not toxic to the liver in this 12-week study.

In conclusion, we show that targeted dual NP therapy of EDTA followed by delivery of PGG is an effective way to reverse moderately developed aortic

aneurysms and elastin calcification. It regenerates elastic lamina and restores healthy elastic lamina in an experimental rat model of aortic aneurysms. Thus, such therapies could be promising approach for patients diagnosed with moderate-level AAA disease.

## Clinical Implementation

Over 90 percent of AAA are diagnosed at an early stage with no known treatment. Patients are on watchful eye and monitored for AAA expansion. This novel targeted systemic therapy can be used to stop the expansion of the dilated vessel, and restore vessel homeostasis. Such therapy will prolong or eliminate risky vascular graft surgery in elderly.

## Acknowledgments

We would like to acknowledge Clemson University's Godley-Snell Research Center for help with the animal studies. We would like to acknowledge Jenny Bourne for help with editing the manuscript.

## Sources of Funding

We gratefully acknowledge funding from the NIH grant P20GM103444 and the Hunter Endowment at Clemson University to (NV).

## Competing Interests

The authors have declared that no competing interest exists.

## References

- Kent KC. Abdominal aortic aneurysms. *N Engl J Med*. 2014; 371: 2101-8.
- Assar AN, Zarins C. Ruptured abdominal aortic aneurysm: a surgical emergency with many clinical presentations. *Postgraduate medical journal*. 2009; 85: 268-73.
- Ishizaka N, Sohmiya K, Miyamura M, Umeda T, Tsuji M, Katsumata T, et al. Infected aortic aneurysm and inflammatory aortic aneurysm—in search of an optimal differential diagnosis. *Journal of cardiology*. 2012; 59: 123-31.
- Mäyränpää MI, Trosien JA, Fontaine V, Folkesson M, Kazi M, Eriksson P, et al. Mast cells associate with neovessels in the media and adventitia of abdominal aortic aneurysms. *Journal of vascular surgery*. 2009; 50: 388-95.
- Li Z-Y, Jean U, Tang TY, Soh E, See TC, Gillard JH. Impact of calcification and intraluminal thrombus on the computed wall stresses of abdominal aortic aneurysm. *Journal of vascular surgery*. 2008; 47: 928-35.
- Miyake T, Morishita R. Pharmacological treatment of abdominal aortic aneurysm. *Cardiovascular research*. 2009; cyp155.
- Wang Y, Krishna S, Gollidge J. The calcium chloride-induced rodent model of abdominal aortic aneurysm. *Atherosclerosis*. 2013; 226: 29-39.
- Nosoudi N, Nahar-Gohad P, Sinha A, Chowdhury A, Gerard P, Carsten CG, et al. Prevention of Abdominal Aortic Aneurysm Progression by Targeted Inhibition of Matrix Metalloproteinase Activity with Batimastat-Loaded Nanoparticles. *Circulation research*. 2015; 117: e80-e9.
- Lei Y, Nosoudi N, Vyavahare N. Targeted chelation therapy with EDTA-loaded albumin nanoparticles regresses arterial calcification without causing systemic side effects. *Journal of Controlled Release*. 2014; 196: 79-86.
- Buijs R, Willems T, Tio R, Boersma H, Tielliu I, Slart R, et al. Calcification as a risk factor for rupture of abdominal aortic aneurysm. *European Journal of Vascular and Endovascular Surgery*. 2013; 46: 542-8.
- Isenburg JC, Simionescu DT, Starcher BC, Vyavahare NR. Elastin stabilization for treatment of abdominal aortic aneurysms. *Circulation*. 2007; 115: 1729-37.
- Merodio M, Arnedo A, Renedo MJ, Irache JM. Ganciclovir-loaded albumin nanoparticles: characterization and in vitro release properties. *European Journal of Pharmaceutical Sciences*. 2001; 12: 251-9.
- Chiou AC, Chiu B, Pearce WH. Murine aortic aneurysm produced by periarterial application of calcium chloride. *Journal of Surgical Research*. 2001; 99: 371-6.

- Choudhary B, Zhou J, Li P, Thomas S, Kaartinen V, Sucov HM. Absence of TGF $\beta$  signaling in embryonic vascular smooth muscle leads to reduced lysyl oxidase expression, impaired elastogenesis, and aneurysm. *Genesis*. 2009; 47: 115-21.
- Nasim Nosoudi AC, Steven Siclari, Vaideesh Parasaram, Saketh Karamched, Naren R. Vyavahare. Systemic delivery of nanoparticles loaded with pentagalloyl glucose protects elastic lamina and prevents abdominal aortic aneurysm in rats, *Cardiovascular Translational Research*. (under review).
- O'Leary SA, Mulvihill JJ, Barrett HE, Kavanagh EG, Walsh MT, McGloughlin TM, et al. Determining the influence of calcification on the failure properties of abdominal aortic aneurysm (AAA) tissue. *Journal of the mechanical behavior of biomedical materials*. 2015; 42: 154-67.
- Seely DM, Wu P, Mills EJ. EDTA chelation therapy for cardiovascular disease: a systematic review. *BMC Cardiovascular Disorders*. 2005; 5: 32.
- Lamas GA, Goertz C, Boineau R, Mark DB, Rozema T, Nahin RL, et al. Design of the trial to assess chelation therapy (TACT). *American heart journal*. 2012; 163: 7-12.
- Luck G, Liao H, Murray NJ, Grimmer HR, Warminski EE, Williamson MP, et al. Polyphenols, astringency and proline-rich proteins. *Phytochemistry*. 1994; 37: 357-71.
- Scrutton MC. Proteinmetal interactions. *FEBS Letters*. 1976; 70: 291-2.
- Giachelli CM, Speer MY, Li X, Rajachar RM, Yang H. Regulation of vascular calcification roles of phosphate and osteopontin. *Circulation Research*. 2005; 96: 717-22.
- Pei H, Tian C, Sun X, Qian X, Liu P, Liu W, et al. Overexpression of MicroRNA-145 Promotes Ascending Aortic Aneurysm Media Remodeling through TGF- $\beta$ 1. *European Journal of Vascular and Endovascular Surgery*. 2015; 49: 52-9.
- Gabriel EA, Gabriel SA. *Inflammatory Response in Cardiovascular Surgery*: Springer; 2013.
- Guo G, Gehle P, Doelken S, Martin-Ventura JL, Von Kodolitsch Y, Hetzer R, et al. Induction of macrophage chemotaxis by aortic extracts from patients with Marfan syndrome is related to elastin binding protein. *PLoS One*. 2011; 6: e20138.
- Nakazato Y, Yamaji Y, Oshima N, Hayashi M, Saruta T. Calcification and osteopontin localization in the peritoneum of patients on long-term continuous ambulatory peritoneal dialysis therapy. *Nephrology Dialysis Transplantation*. 2002; 17: 1293-303.
- Yamanouchi D, Morgan S, Stair C, Seedial S, Lengfeld J, Kent KC, et al. Accelerated aneurysmal dilation associated with apoptosis and inflammation in a newly developed calcium phosphate rodent abdominal aortic aneurysm model. *Journal of vascular surgery*. 2012; 56: 455-61.
- Sun J, Sukhova GK, Yang M, Wolters PJ, MacFarlane LA, Libby P, et al. Mast cells modulate the pathogenesis of elastase-induced abdominal aortic aneurysms in mice. *The Journal of clinical investigation*. 2007; 117: 3359-68.
- Sinha A NN, Vyavahare N. Elasto-regenerative properties of polyphenols. *Biochemical and Biophysical Research Communications Biochemical and Biophysical Research Communications*. 2014; 444: 205-11.
- Kothapalli CR, Ramamurthi A. Lysyl oxidase enhances elastin synthesis and matrix formation by vascular smooth muscle cells. *Journal of tissue engineering and regenerative medicine*. 2009; 3: 655-61.
- Rowe DW, McGoodwin EB, Martin GR, Grahn D. Decreased lysyl oxidase activity in the aneurysm-prone, mottled mouse. *Journal of Biological Chemistry*. 1977; 252: 939-42.
- Mäki JM, Räsänen J, Tikkanen H, Sormunen R, Mäkiöllinen K, Kivirikko KI, et al. Inactivation of the lysyl oxidase gene *Lox* leads to aortic aneurysms, cardiovascular dysfunction, and perinatal death in mice. *Circulation*. 2002; 106: 2503-9.
- Krettek A, Sukhova GK, Libby P. Elastogenesis in Human Arterial Disease A Role for Macrophages in Disordered Elastin Synthesis. *Arteriosclerosis, thrombosis, and vascular biology*. 2003; 23: 582-7.
- Carmo M, Colombo L, Bruno A, Corsi F, Roncoroni L, Cuttin M, et al. Alteration of elastin, collagen and their cross-links in abdominal aortic aneurysms. *European journal of vascular and endovascular surgery*. 2002; 23: 543-9.
- Favreau JT, Nguyen BT, Gao I, Yu P, Tao M, Schneiderman J, et al. Murine ultrasound imaging for circumferential strain analyses in the angiotensin II abdominal aortic aneurysm model. *Journal of vascular surgery*. 2012; 56: 462-9.
- Liu L, Hitchens TK, Ye Q, Wu Y, Barbe B, Prior DE, et al. Decreased reticuloendothelial system clearance and increased blood half-life and immune cell labeling for nano- and micron-sized superparamagnetic iron-oxide particles upon pre-treatment with Intralipid. *Biochimica et Biophysica Acta (BBA)-General Subjects*. 2013; 1830: 3447-53.
- Venkatasubbu GD, Ramasamy S, Gaddam PR, Kumar J. Acute and subchronic toxicity analysis of surface modified paclitaxel attached hydroxyapatite and titanium dioxide nanoparticles. *International journal of nanomedicine*. 2015; 10: 137.